Published in final edited form as:
Biomaterials. 2011 August ; 32(22): 5023–5032. doi:10.1016/j.biomaterials.2011.03.070.

Induced Pluripotent Stem Cells for Neural Tissue Engineering

Aijun Wang[1], **Zhenyu Tang**[1], **In-Hyun Park**[2,*], **Yiqian Zhu**[1], **Shyam Patel**[3], **George Q. Daley**[2], and **Li Song**[1,§]

[1]Department of Bioengineering, University of California, Berkeley

[2]Stem Cell Transplantation Program, Division of Pediatric Hematology/Oncology, Manton Center for Orphan Disease Research, Howard Hughes Medical Institute, Children's Hospital Boston and Dana Farber Cancer Institute; Division of Hematology, Brigham and Women's Hospital; Department of Biological Chemistry and Molecular Pharmacology, Harvard Medical School; Harvard Stem Cell Institute; Boston, MA 02115, USA

[3]Nanonerve Inc.

Abstract

Induced pluripotent stem cells (iPSCs) hold great promise for cell therapies and tissue engineering. Neural crest stem cells (NCSCs) are multipotent and represent a valuable system to investigate iPSC differentiation and therapeutic potential. Here we derived NCSCs from human iPSCs and embryonic stem cells (ESCs), and investigated the potential of NCSCs for neural tissue engineering. The differentiation of iPSCs and the expansion of derived NCSCs varied in different cell lines, but all NCSC lines were capable of differentiating into mesodermal and ectodermal lineages, including neural cells. Tissue-engineered nerve conduits were fabricated by seeding NCSCs into nanofibrous tubular scaffolds, and used as a bridge for transected sciatic nerves in a rat model. Electrophysiological analysis showed that only NCSC-engrafted nerve conduits resulted in an accelerated regeneration of sciatic nerves at 1 month. Histological analysis demonstrated that NCSC transplantation promoted axonal myelination. Furthermore, NCSCs differentiated into Schwann cells and were integrated into the myelin sheath around axons. No teratoma formation was observed for up to 1 year after NCSC transplantation in vivo. This study demonstrates that iPSC-derived multipotent NCSCs can be directly used for tissue engineering and that the approach that combines stem cells and scaffolds has tremendous potential for regenerative medicine applications.

Keywords

Stem cells; scaffold; nerve guide; nerve tissue engineering; nanofibers; neural crest stem cell

INTRODUCTION

Cell source is a major issue for tissue engineering and regenerative medicine. An exciting breakthrough in stem cell biology is that adult somatic cells (e.g., skin fibroblasts) can be reprogrammed into induced pluripotent stem cells (iPSCs) by the activation of a limited number of genes (transgenes) such as Oct3/4, Sox2, c-Myc and KLF4 [1, 2] or Oct3/4, Sox2, Nanog and Lin28 [3]. The iPSCs derived from somatic cells make it possible for patient-specific cell therapies, which bypasses immune rejection issue and ethical concerns

[§]Corresponding address: Song Li, Ph.D., Department of Bioengineering, University of California, Berkeley, B108A Stanley Hall, Berkeley, CA 94720-1762, Telephone: (510) 666-2799, Fax: (510) 666-3381, song_li@berkeley.edu.
[*]Current address: Department of Genetics, Yale School of Medicine

of deriving and using embryonic stem cells (ESCs) as a cell source. The unlimited expansion potential of iPSCs also makes them a valuable cell source for tissue engineering. However, to use iPSCs as a cell source, many important issues remain to be addressed, such as the differences among various iPSC lines in differentiation and expansion and the appropriate differentiation stage of the cells for specific tissue engineering applications. Neural crest stem cells (NCSCs) can differentiate into cell types of all three germ layers, and represent a valuable model system to investigate the differentiation and therapeutic potential of stem cells [4–8]. Here we derived NCSCs from human iPSCs and ESCs to determine the variation among iPSC lines, and used the model of peripheral nerve regeneration to investigate the differentiation and therapeutic potential of NCSCs *in vivo*.

Nerve conduits are usually used to bridge transected peripheral nerves [9, 10]; however, the regeneration is often limited and slow [11–14]. There is evidence that the transplantation of Schwann cells or precursor cells derived from skin or other adult tissues can facilitate nerve regeneration [15, 16], but adult cell sources are limited by the number of cells that can be obtained and complicated by the need to sacrifice additional nerves and tissues. Moreover, there is a lack of efficiency and consistency in cell isolation and expansion, which causes variability in therapeutic efficacy. In contrast, NCSCs derived from iPSCs can be immune compatible, expandable, and well characterized as a valuable cell source for the regeneration of peripheral nerve and other tissues.

MATERIALS AND METHODS

(Details can be found in Supplemental Methods)

Cell Culture, NCSC Derivation and Differentiation

Undifferentiated human iPSCs (passages 22–45) and hESC lines H1 and H9 (WiCell Research Institute; passages 30–50) were maintained as described previously [17]. To derive NCSCs, iPSCs and ESCs were detached by collganase IV (1 mg/ml) and dispase (0.5 mg/ml), and grown as embryo body (EB)-like floating cell aggregates in ESC maintenance medium without bFGF for 5 days. The cell aggregates were allowed to adhere to CELLstart matrix (Invitrogen) coated dishes in a serum-free neural induction medium (SFM) consisting of Knockout DMEM/F12, StemPro neural supplement (Invitrogen), 1% GlutaMAX™-I (Invitrogen), 20 ng/ml bFGF and 20 ng/ml EGF. After 7 more days, the colonies with rosette structures were mechanically harvested, cultured in suspension in SFM medium for one week, replated onto CellStart coated dishes, and cultured for 3 more days. Cells were dissociated into single cells by TryplE Select (Invitrogen) and cultured in SFM medium in ultra low attachment tissue culture plates (Costar) for one more week. The secondary spheres formed in suspension were collected and replated on CellStart-coated dishes in SFM medium. Cells were allowed to migrate out of the attached secondary spheres and grow to confluence; then the cells were dissociated and cultured as a monolayer. NCSC lines that were homogeneously positive for p75 were selected for further studies. Some of the cell lines were further purified by FACS for p75+ cells to obtain homogeneous populations that were positive for p75, HNK1 and AP2. The cells were maintained in SFM on CellStart-coated dishes with 50% of the medium changed every 2 days, and were passaged weekly. To test the multipotency of NCSCs, cell differentiation into neural cells and mesenchymal cells was carried out using the protocol described previously [7, 18].

Biochemical Analysis

Immunostaining, microscopy, real-time polymerase chain reaction (PCR) and flow cytometry analysis were performed as described previously [18, 19].

Scaffold Fabrication

Electrospinning technique was used to produce nanofibrous nerve conduits. Nonwoven aligned nanofibrous nerve conduits composed of poly(L-lactide-co-caprolactone) (70:30, Purac Biomaterials, Amsterdam, Netherlands), poly(propylene glycol) (Acros Organics, Morris Plains, NJ) and sodium acetate (Sigma, St. Louis, MO) were fabricated by using a customized electrospinning process. To make tubular scaffolds with aligned nanofibers in the longitudinal direction on luminal surface, a rotating mandrel assembly with two electrically conductive ends and a central non-conductive section was used. The jet stream of polymer solution from the spinneret whipped between the two conductive ends, resulting in longitudinally aligned nanofibers forming a tubular scaffold on the non-conductive portion of the mandrel. To enhance the mechanical strength of the scaffolds, outer layers of random nanofibers were deposited on this layer of longitudinally aligned fibers.

Tissue Engineered Conduits and In Vivo Transplantation

The nerve conduits were sterilized by ethylene oxide gas sterilization before use. NCSCs were detached and re-suspended in SFM ($2–3 \times 10^4$ cells/μl). The cell suspension was mixed with a cold matrigel solution at a 2:1 ratio (volume to volume), and injected into the nanofibrous nerve conduits (e.g., 45 μl for one conduit 1.2 cm in length). The tissue-engineered constructs were kept in the incubator for one hour, and NCSC maintenance medium was added to cover the constructs. The culture was maintained in the incubator overnight before surgery. Live/Dead assay (Molecular Probes) was used to assess the viability of the NCSCs in the tissue-engineered nerve conduits.

All experimental procedures with animals were approved by the ACUC committee at UC Berkeley and were carried out according to the institutional guidelines. Adult female athymic rats (National Cancer Institute) weighing 200–250 g were used in all experiments. Three experimental groups were included: (1) conduits filled with matrigel (diluted with SFM at a 1:2 ratio) without cells (as control, 10 animals), (2) conduits seeded with NCSCs derived from iPSCs (4 iPSC lines: BJ1-iPS1, ADAfE4-iPS38, dH1f-iPS2-2, MSC-iPS1; 6 animals for each cell line), and (3) conduits seeded with NCSCs derived from hESCs (H1 and H9 cell lines).

The sciatic nerve was severed with a scalpel, and 0.6 cm of the nerve trunk was cut off. A nerve conduit (1.2 cm in length) was inserted between the two nerve stumps and sutured under the microscope with 9–0 sutures, creating a gap of 1 cm between the two stumps.

Electrophysiology

To directly evaluate the regeneration of the sciatic nerve across the conduits, electrophysiology testing was performed before euthanasia. Electrical stimuli (1 mA in strength) were applied to the native sciatic nerve trunk at the point 5-mm proximal to the graft suturing point, and CMAPs were recorded on the gastrocnemius belly. Normal CMAPs from the un-operated contralateral side of sciatic nerve were also recorded for comparison.

Histological Analysis

After electrophysiology testing, the nerve conduits were explanted and fixed in 4% paraformaldehyde at 4°C. Longitudinal sections (12 μm in thickness) and cross sections in the middle portion of the graft (10 μm in thickness; 5–7 mm from the proximal end of the graft) were cryosectioned for H&E staining and immunostaining.

Evaluation of Myelination

The nerve conduits were explanted, and nerve cross-sections at the middle portion of the graft (5–7 mm from the proximal end) were processed and stained by toluidine blue for myelin sheath. Briefly, the samples were fixed, mounted in embedding resin, sectioned at 800 nm thickness with a microtome, and stained with 1% toluidine blue. The total number of myelinated axons per unit area was quantified by using ImageJ software.

RESULTS

Derivation and Characterization of NCSCs from iPSCs and hESCs

We derived NCSCs from ESCs or iPSCs as described in Figure 1***A***. To derive NCSCs, hESCs and iPSCs were first cultured as cell aggregates in suspension, and then allowed to adhere to form rosette structures (Figure 1 ***B***) for NCSC isolation. Two human ESC lines (H1 and H9) robustly differentiated into NCSCs. Out of seven human iPSC lines tested, MRC5-iPS7 (derived from MRC5 human fetal lung fibroblasts) and hFib2-iPS4 cells (derived from skin fibroblasts) [2] did not differentiate effectively and maintained an undifferentiated ESC/iPSC morphology (Figure 1 ***C, D***), while the other five iPSC lines gave rise to NCSCs. For these five iPSC lines, three were derived from skin fibroblasts (BJ1-iPS1, ADAfE4-iPS38, ADAfE4-iPS38-2), one was derived from H1-OGN differentiated fibroblasts (dH1f-iPS2-2), and one was derived from bone marrow mesenchymal stem cells (MSC-iPS1) [2]. These results suggest that the differentiation of different iPSC lines might vary.

At the rosette stage of ESC and iPSC differentiation, four types of colonies were observed, i.e., colonies with rosette structure (Figure 1***B***), colonies with differentiated neurons (Figure 1 ***E, H***), colonies with myofibroblasts that were positive for smooth muscle α-actin (Figure 1 ***F, I***), and a small number of undifferentiated colonies that were positive for Oct3/4 (Figure 1 ***G, J***). The percentage of each type of colonies for each ESC/iPSC line is summarized in Supplementary Figure 1. Some iPSC lines (BJ1-iPS1, MSC-iPS1, ADAfE4-iPS38-2) and ESC line (H9) formed more colonies with the rosette structure, whereas other iPSC line (dH1f-iPS2-2, ADAfE4-iPS38) and ESC line (H1) had lower number of colonies with rosettes.

Although different iPSC and ESC lines had different efficiency in forming rosettes, the majority of cells in the colonies with rosette structures were positive for neural crest markers AP2, nestin and p75 (Figure 1 ***K–M***). ESC and iPSC colonies with rosette structures were mechanically harvested, cultured in suspension, and transferred to monolayer culture. Flow cytometry analysis of the cells showed that 80–95% of cells were p75+/HNK1+ (Supplemental Figure 2) in different NCSC lines. The gene expression at different stages of the differentiation process was characterized. ESCs (as exemplified in Figure 2***A***) lost the expression of pluripotency markers Oct3/4 and Nanog upon differentiation. The expression of mesoderm marker T-Brachyury and endoderm marker FoxA2 also decreased. In contrast, the expression of various neural crest markers including AP2, Sox10, Slug and Brn3a significantly increased during the differentiation process (Figure 2***B***). The expression of the reprogramming genes as well as the neural crest markers was characterized during the differentiation of ESCs and iPSCs. The expression of Oct3/4 and Sox2 decreased significantly while the expression of c-Myc and Klf4 varied among the different cell lines (Figure 2 ***C–F***). In parallel, the expression of neural crest markers AP2 and Slug increased dramatically (Figure 2 ***G–H***).

During cell maintenance and expansion, NCSCs became more homogeneous in most of the cell lines as shown by the expression of NCSC markers nestin and AP2, p75, and HNK1. Homogeneous NCSC lines were selected for further studies. For the cell lines with a less

homogeneous population, cells were further purified by fluorescence-activated cell sorting (FACS) for p75+ cells, and verified by positive staining of p75, HNK1 and AP2. As exemplified in Figure 3, an iPSC (BJ1-iPS1)-derived NCSC line (iPSC-NCSCs) and an ESC (H1)-derived NCSC line (ESC-NCSCs) homogeneously expressed NCSC markers nestin, AP2, p75 and HNK1 (Figure 3 ***A–H***). In addition, both ESC-NCSCs and iPSC-NCSCs formed neural sphere-like aggregates when cultured on ultra-low-attachment plates in the presence of basic fibroblast growth factor (bFGF) and epidermal growth factor (EGF), and the cells within the spheres retained the expression of NCSC markers nestin, vimentin, p75 and HNK1 (Figure 3 ***I–P***).

Expansion and Differentiation Potential of Derived NCSCs

All NCSC lines from ESCs and iPSCs were expandable for at least 8 passages. However, there were significant differences in cell doubling time during cell expansion (Supplemental Figure 3). NCSCs derived from MSC-iPS1 and H1 ESCs grew much faster than other NCSC lines, with a cell doubling time between 40 and 45 hours. NCSCs derived from other cell lines had a doubling time between 75 and 96 hours. Next we assessed the differentiation of ESC-and iPSC-derived NCSCs into mesodermal and ectodermal lineages. All NCSC lines, regardless of differences in growth rate, were capable of differentiating into the mesodermal and ectodermal lineages. Representative results for iPSC-NCSCs are shown in Figure 4. Neuronal differentiation was induced by the combination of BDNF, GDNF, NGF and dibutyryl cyclic AMP (dbcAMP) [7]. After 2 weeks, NCSCs differentiated into peripheral neurons positive for Tuj1 and peripherin (Figure 4 ***A–B***). GFAP+/S100β+ Schwann cells were induced by CNTF, neuregulin 1β and dbcAMP (Figure 4 ***C–D***). Peripheral neurons had multiple neurites, and Schwann cells had long and thin protrusions (Supplemental Figure 4 ***A–B***). However, these peripheral neurons and Schwann cells were not expandable, detached from culture surfaces easily, and had a low survival rate in culture, which made them unsuitable for therapeutic applications. Besides the peripheral neural lineages, NCSCs could also differentiate into various mesenchymal lineages. Under specific conditions [7, 18], ESC-NCSCs and iPSC-NCSCs differentiated into chondrocytes, osteoblasts, adipocytes and smooth muscle precursors (Figure 4 ***E–L***). These results demonstrated the multipotency of the NCSCs.

Construction of Tissue Engineered-Nerve Conduits

To explore the potential of iPSC-derived NCSCs for tissue engineering applications, we constructed tissue-engineered nerve conduits for the regeneration of the transected sciatic nerve in a rat model. The tissue engineering approach is schematically outlined in Figure 5 ***A***. Our previous studies have shown that aligned nanofibers can provide topographical guidance to accelerate axon growth and cell migration *in vitro* [20, 21]. Long term *in vivo* studies also showed that nanofibrous nerve conduits with longitudinally aligned nanofibers had comparable therapeutic effects to autografts for nerve regeneration, with a partial functional recovery after 2 months [22]. We engineered the electrospinning system to fabricate bilayered nanofibrous nerve conduits by using the biodegradable polymer poly(L-lactide-co-caprolactone), with longitudinally aligned nanofibers on the luminal surface. The outer layer of the nerve conduits had randomly oriented nanofibers, which provided sufficient mechanical strength for the conduits. NCSCs (passage 4) derived from iPSCs or ESCs were mixed with matrigel, and delivered into the lumen of the conduits. A cell viability assay showed that >90% of the cells survived in the nerve conduits after 1-day of *in vitro* culture (Figure 5 ***B–C***). These tissue-engineered nerve conduits were maintained in a cell culture incubator for one day at 37°C before being used for nerve repair.

The Effect of NCSC-Grafted Nerve Conduits on Nerve Regeneration

The sciatic nerve in rats was transected, and the gap (1 cm) was bridged by a tissue-engineered nerve conduit, with or without NCSCs. The nerve conduit formed a well-controlled microenvironment for the study of NCSC differentiation and function in the regenerating nerve. After 1 month, electrophysiological tests were performed to examine the regeneration of sciatic nerves in the animals. Compound muscle action potentials (CMAPs) were recorded at both the operated and un-operated (normal) sides for each animal. CMAPs were detected from all the animals in the NCSC-engrafted groups (36 rats, including 6 rats for each of the four iPSC-NCSC lines and two ESC-NCSC lines), while CMAPs were not detected in the conduit-alone control group (10 rats, grafted with conduits filled with matrigel without cells) (Figure 6 ***A–C***), suggesting that NCSCs were capable of accelerating the regeneration of peripheral nerves. The magnitude of CMAPs in the NCSC-engrafted group at 1 month was about one-third of a normal sciatic nerve (Figure 6 ***D***).

The Mechanism of NCSC-Promoted Nerve Regeneration

To elucidate the mechanism by which NCSCs promoted the regeneration of peripheral nerves, we performed extensive histological analysis. Hematoxylin and eosin (H&E) staining of the longitudinally sectioned samples revealed that peripheral nerve tissue grew across the nerve conduits in both the NCSC-engrafted group and conduit-alone group (Figure 7 ***A–B***). Immunostaining for the axon marker neurofilament M subunit (NF-M) and the Schwann cell marker S100β in the cross sections of regenerated sciatic nerve revealed that the NCSC-engrafted group had regenerated both a greater number of axons and more Schwann cells around individual axons than the conduit alone group (Figure 7 ***C–D***). Schwann cells enveloping axons in NCSC-engrafted nerves were visible at high magnification (Figure 7 ***E***). Toluidine blue staining of the cross sections revealed a significant increase in myelinated axons in the setting of NCSC transplantation (Figure 7 ***F–H***). These results indicated that the transplanted NCSCs enhanced the regeneration of peripheral nerves by facilitating the myelination of regenerating axons.

We then examined the fate of transplanted NCSCs in the regenerated nerve to determine whether engrafted cells contributed to the myelination of axon. Human nuclear mitotic apparatus protein (NuMA) was used to identify the transplanted cells in histological analysis. Longitudinal sections of the nerve conduits were double-stained for NuMA and the Schwann cell specific marker S100β. One-month after transplantation, the transplanted human iPSC-NCSCs were viable and were positive for Schwann cell marker S100β (Figure 7 ***I***). NuMA/S100β positive cells were clearly integrated into the myelin sheath around axons (Figure 7 ***J***). We found no evidence that NCSCs differentiated into neurons, and there was no teratoma formation following NCSC transplantation for up to 1 year.

DISCUSSION

In general, most of iPSC lines, as ESCs, can differentiate into NCSCs, although the differentiation efficiency was different. We classified colonies at the rosette stage into four types and used this classification to evaluate the differentiation efficiency. The percentage of the four types of colonies (i.e. rosettes, undifferentiated colonies, differentiated colonies with neurons and differentiated colonies with myofibroblasts) was quite different for each iPSC and ESC line (Supplemental Figure 1). These results suggest that differentiation efficiency is an important variable for both ESCs and iPSCs. In addition, two of the iPSC lines remained undifferentiated and failed to form rosettes. This may be related to the reactivation of reprogramming factors upon differentiation [23], or represent a consequence of stochastic differences in reprogramming [24]. Therefore, it is critical to select appropriate iPSC lines as cell sources for tissue engineering.

Furthermore, there was a substantial difference in the expansion potential of NCSCs derived from iPSCs and ESCs. At early passages, the difference in expansion potential was reflected in cell doubling time that varied for each iPSC or ESC line, but there was no clear trend to distinguish iPSC-NCSCs from ESC-NCSCs. Interestingly, the cell doubling time for different NCSC lines derived from the same iPSC or ESC line was similar, suggesting that this is dependent on the iPSC or ESC line rather than different clones of NCSCs. In animal studies, we did not observe teratoma formation for up to 1 year after transplantation, suggesting that it is safe to use iPSC-NCSCs for tissue engineering.

Our results also indicate that NCSC is an appropriate cell type and a valuable cell source for tissue repair. In regenerating nerves, NCSCs differentiated into Schwann cells and became integrated into the myelin sheath around axons, which enhanced myelination and the regeneration of peripheral nerves. This therapeutic effect was specific for NCSCs, as NCSC-derived myofibroblasts did not produce a similar anatomic or therapeutic effect (unpublished data). Since mature neurons and Schwann cells have low survival rates in culture, NCSCs are more appropriate for tissue engineering applications.

NCSCs preferentially differentiated into Schwann cells in our peripheral nerve regeneration studies, suggesting that NCSC differentiation *in vivo* may be guided by the microenvironmental factors in specific tissues. However, any clinical use of NCSCs would require an exhaustive evaluation of their potential for aberrant differentiation into unwanted lineages, which might complicate their therapeutic utility. Should the microenvironment prove dominant in defining the *in vivo* fate of NCSCs, as suggested in our studies, the use of multipotent stem cells such as NCSCs in tissue engineering represents an exciting strategy for the regeneration of tissues and organs.

CONCLUSION

Induced pluripotent stem cells and their derivatives are valuable cell sources for tissue engineering. The efficiency of deriving specific cells from iPSCs may vary for each cell line. A strategy is to derive expandable multipotent stem cells such as NCSCs from iPSCs and use NCSCs or further differentiated cells for therapies. This study shows that NCSCs derived from iPSCs and ESCs have similar characteristics and therapeutic effects on nerve regeneration. Multipotent NCSCs can be directly used for tissue repair as exemplified in nerve regeneration. Specifically, NCSCs differentiated into Schwann cells and facilitate the myelination of axons, thus promoting nerve regeneration. Furthermore, this study demonstrates that combining stem cells and engineered scaffolds results in superior therapeutic effect and this approach has tremendous potential for regenerative medicine and tissue engineering applications.

Supplementary Material

Refer to Web version on PubMed Central for supplementary material.

Acknowledgments

This work was supported in part by the grants from National Institute of Health (EB012240 and HL083900 to S.L., HL102815 and HL100001 to G.Q.D.), Manton Center for Orphan Diseases (to G.Q.D.), the Howard Hughes Medical Institute (to G.Q.D.), and a postdoctoral training grant TG2-01164 from California Institute for Regenerative Medicine (to A.W.).

REFERENCES

1. Takahashi K, Tanabe K, Ohnuki M, Narita M, Ichisaka T, Tomoda K, et al. Induction of pluripotent stem cells from adult human fibroblasts by defined factors. Cell. 2007; 131:861–872. [PubMed: 18035408]
2. Park IH, Zhao R, West JA, Yabuuchi A, Huo H, Ince TA, et al. Reprogramming of human somatic cells to pluripotency with defined factors. Nature. 2008; 451:141–146. [PubMed: 18157115]
3. Yu J, Vodyanik MA, Smuga-Otto K, Antosiewicz-Bourget J, Frane JL, Tian S, et al. Induced pluripotent stem cell lines derived from human somatic cells. Science. 2007; 318:1917–1920. [PubMed: 18029452]
4. Rao MS, Anderson DJ. Immortalization and controlled in vitro differentiation of murine multipotent neural crest stem cells. J Neurobiol. 1997; 32:722–746. [PubMed: 9183749]
5. Morrison SJ, White PM, Zock C, Anderson DJ. Prospective identification, isolation by flow cytometry, and in vivo self-renewal of multipotent mammalian neural crest stem cells. Cell. 1999; 96:737–749. [PubMed: 10089888]
6. Crane JF, Trainor PA. Neural crest stem and progenitor cells. Annu Rev Cell Dev Biol. 2006; 22:267–286. [PubMed: 16803431]
7. Lee G, Kim H, Elkabetz Y, Al Shamy G, Panagiotakos G, Barberi T, et al. Isolation and directed differentiation of neural crest stem cells derived from human embryonic stem cells. Nat Biotechnol. 2007; 25:1468–1475. [PubMed: 18037878]
8. Sauka-Spengler T, Bronner-Fraser M. A gene regulatory network orchestrates neural crest formation. Nat Rev Mol Cell Bio. 2008; 9:557–568. [PubMed: 18523435]
9. Wang AJ, Ao Q, Cao WL, Yu MZ, He Q, Kong LJ, et al. Porous chitosan tubular scaffolds with knitted outer wall and controllable inner structure for nerve tissue engineering. J Biomed Mater Res A. 2006; 79A:36–46. [PubMed: 16758450]
10. Wang AJ, Ao Q, Wei YJ, Gong K, Liu XS, Zhao NN, et al. Physical properties and biocompatibility of a porous chitosan-based fiber-reinforced conduit for nerve regeneration. Biotechnol Lett. 2007; 29:1697–1702. [PubMed: 17628751]
11. Schmidt CE, Leach JB. Neural tissue engineering: Strategies for repair and regeneration. Annu Rev Biomed Eng. 2003; 5:293–347. [PubMed: 14527315]
12. Belkas JS, Shoichet MS, Midha R. Peripheral nerve regeneration through guidance tubes. Neurol Res. 2004; 26:151–160. [PubMed: 15072634]
13. Bellamkonda RV. Peripheral nerve regeneration: An opinion on channels, scaffolds and anisotropy. Biomaterials. 2006; 27:3515–3518. [PubMed: 16533522]
14. Chew SY, Mi R, Hoke A, Leong KW. Aligned protein-polymer composite fibers enhance nerve regeneration: A potential tissue-engineering platform. Adv Funct Mater. 2007; 17:1288–1296. [PubMed: 18618021]
15. Rodriguez FJ, Verdu E, Ceballos D, Navarro X. Nerve guides seeded with autologous schwann cells improve nerve regeneration. Exp Neurol. 2000; 161:571–584. [PubMed: 10686077]
16. Tohill M, Terenghi G. Stem-cell plasticity and therapy for injuries of the peripheral nervous system. Biotechnol Appl Biochem. 2004; 40:17–24. [PubMed: 15270703]
17. Lam H, Patel S, Wong J, Chu J, Lau A, Li S. Localized decrease of β-catenin contributes to the differentiation of human embryonic stem cells. Biochem Biophys Res Commun. 2008; 372:601–606. [PubMed: 18515080]
18. Wang D, Park JS, Chu JS, Krakowski A, Luo K, Chen DJ, et al. Proteomic profiling of bone marrow mesenchymal stem cells upon transforming growth factor β1 stimulation. J Biol Chem. 2004; 279:43725–43734. [PubMed: 15302865]
19. Kurpinski K, Chu J, Hashi C, Li S. Anisotropic mechanosensing by mesenchymal stem cells. Proc Natl Acad Sci U S A. 2006; 103:16095–16100. [PubMed: 17060641]
20. Patel S, Kurpinski K, Quigley R, Gao H, Hsiao BS, Poo MM, et al. Bioactive nanofibers: synergistic effects of nanotopography and chemical signaling on cell guidance. Nano Lett. 2007; 7:2122–2128. [PubMed: 17567179]
21. Zhu YQ, Wang AJ, Shen WQ, Patel S, Zhang R, Young WL, et al. Nanofibrous patches for spinal cord regeneration. Adv Funct Mater. 2010; 20:1433–1440.

22. Zhu Y, Wang A, Patel S, Kurpinski K, Diao E, Bao X, et al. Engineering bi-layer nanofibrous conduits for peripheral nerve regeneration. Tissue Eng Part C Methods. 2011 Mar 8. [Epub ahead of print].

23. Miura K, Okada Y, Aoi T, Okada A, Takahashi K, Okita K, et al. Variation in the safety of induced pluripotent stem cell lines. Nat Biotechnol. 2009; 27:743–745. [PubMed: 19590502]

24. Kurpinski K, Lam H, Chu JL, Wang AJ, Kim A, Tsay E, et al. Transforming growth factor-β and notch signaling mediate stem cell differentiation into smooth muscle cells. Stem Cells. 2010; 28:734–742. [PubMed: 20146266]

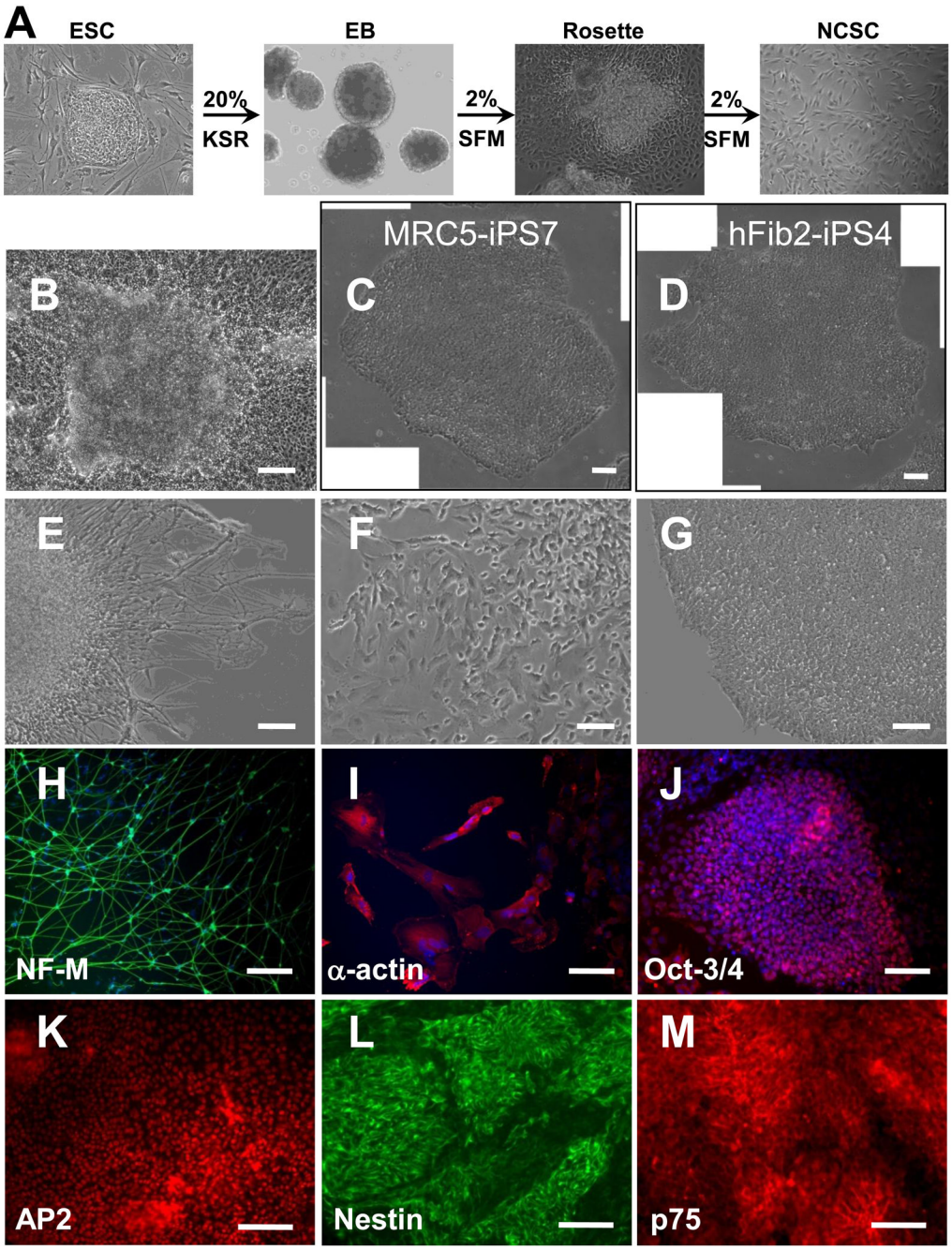

Figure 1.

NCSC derivation from iPSCs and ESCs. (**A**) The procedure to derive NCSCs from iPSCs and ESCs. (**B**) Different iPSC lines behaved differently during differentiation process. Most iPSC and ESC lines formed rosette-like structures during the differentiation process. Two iPSC lines MRC5-iPS7 (derived from MRC5 human fetal lung fibroblasts) and hFib2-iPS4 cells (derived from skin fibroblasts) did not differentiate and maintained undifferentiated ESC/iPSC morphology during the differentiation process (**C, D**). For other ESC and iPSC lines, four types of colonies were identified, i.e., colonies with a rosette structure (**B**), colonies with mature neurons (**E, H**), colonies with myofibroblasts that were positive for smooth muscle α-actin (**F, I**) and a small number of undifferentiated colonies (**G, J**), In the

colonies with rosette structures, the majority of cells were positive for neural crest markers AP2 (**K**), Nestin (**L**) and p75 (**M**). NF-M: Neurofilament M subunit (NF-M). Scale bars in **B, E, F, G, I, J, K, L,** and **M** are 100 μm. Scale bars in **C**, **D**, and **H** are 200 μm.

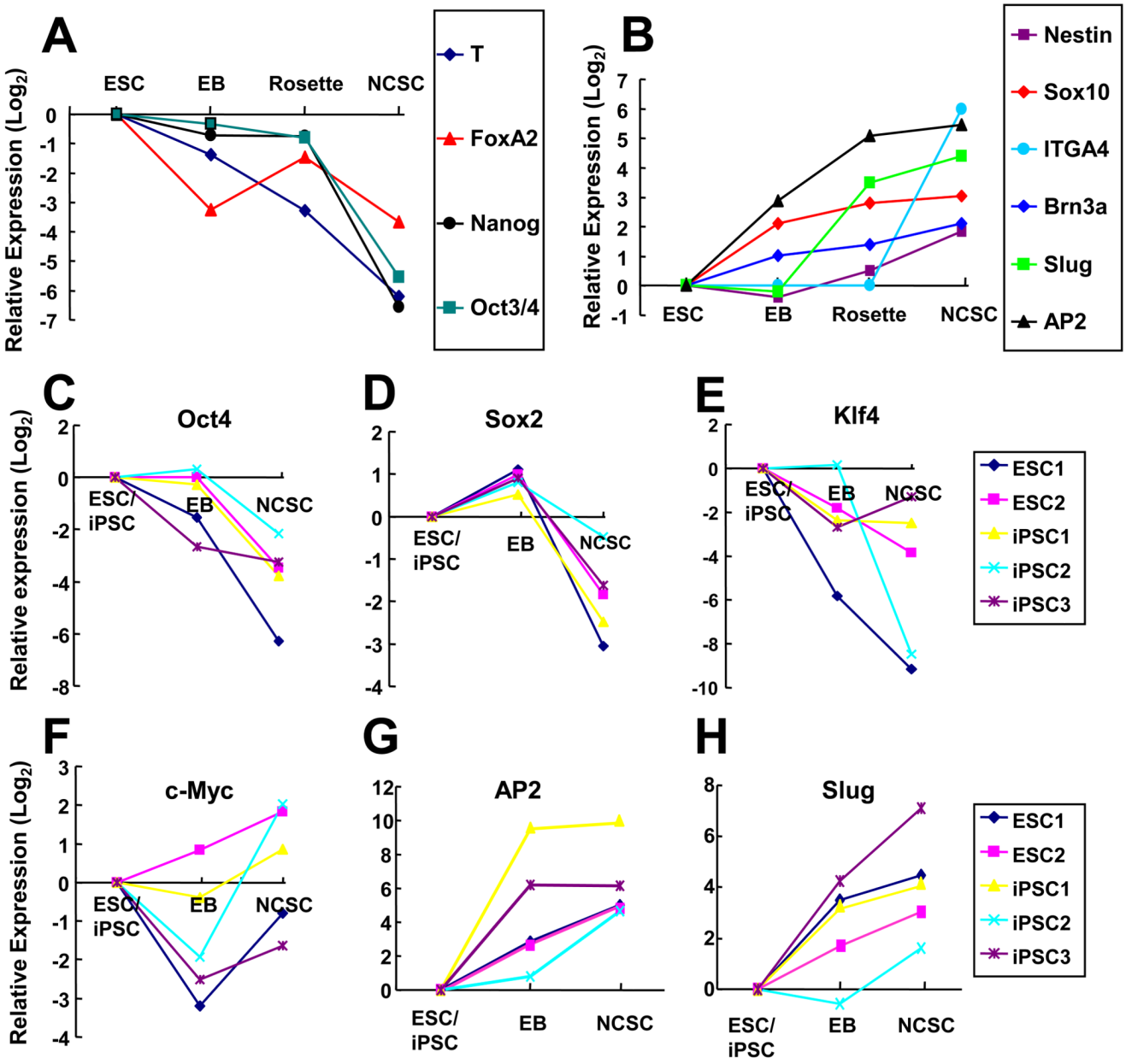

Figure 2.

Gene expression analysis of NCSC derivation process from ESCs and iPSCs. (**A**) Real time PCR analysis of pluripotency markers (Oct3/4 and Nanog), mesoderm marker T-Brachyury and endoderm marker FoxA2 revealed rapid decrease of these markers during the differentiation process. (**B**) Real time PCR analysis of neural crest markers (AP2, Sox10, Slug, ITGA4 and Brn3a) and general neural stem cell marker nestin revealed the differentiation of ESCs (H9) into NCSCs. (**C–H**) Real time PCR analysis of the expression levels of Oct3/4, Sox2, klf4, c-myc, AP2 and Slug during the differentiation of ESCs and iPSCs into NCSCs. In iPSCs, total expression level (including both endogenous and transgenes) was presented. ESC1: H9 cell line. ESC2: H1 cell line. iPSC1: MSC-iPS1 derived from human mesenchymal stem cells. iPSC2: dH1f-iPS2-2 derived from human

fibroblasts (differentiated from H1 human ESCs). iPSC3: ADAfe4-iPS38 derived from human skin fibroblasts.

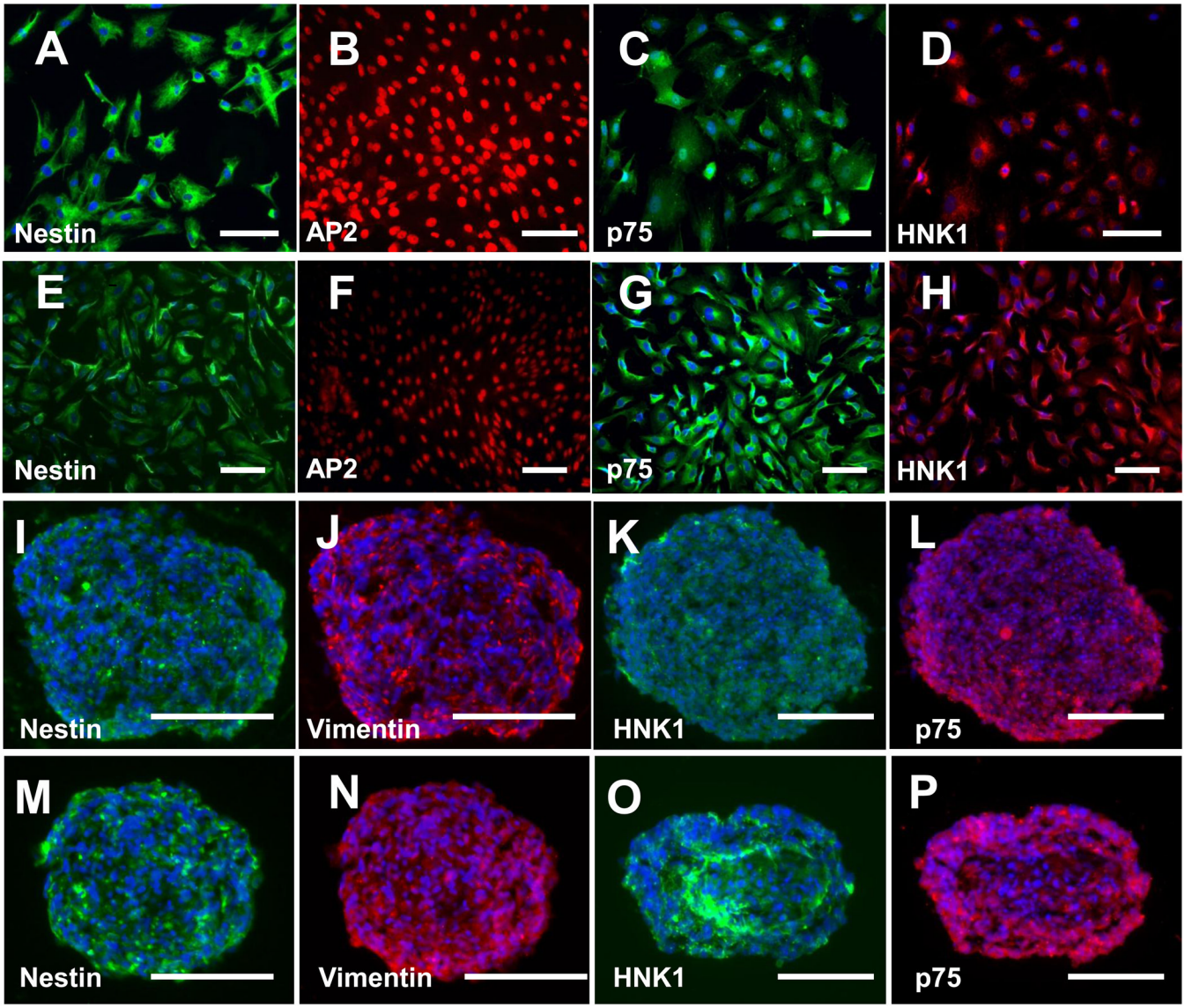

Figure 3.

Characterization of NCSCs derived from iPSCs (iPSC-NCSCs, as exemplified by BJ1-iPS1 line; **A–D** and **I–L**) and hESCs (ESC-NCSCs, as exemplified by H1 line; **E–H** and **M–P**). The ESC-NCSCs and iPSC-NCSCs can be cultured as monolayer in adherent condition (**A–H**). They are stained uniformly for NCSC markers nestin (**A, E**), AP2 (**B, F**), p75 (**C, G**) and HNK1 (**D, H**), indicating their NCSC identity and homogeneity. The ESC-NCSCs and iPSC-NCSCs can also be cultured as floating spheres in low attachment cell culture plates (**I–P**) and maintained uniform expression of NCSC markers nestin (**I, M**), Vimentin (**J, N**), HNK1 (**K, O**) and p75 (**L, P**). Nuclei were stained by DAPI (in blue). Scale bar=100 μm.

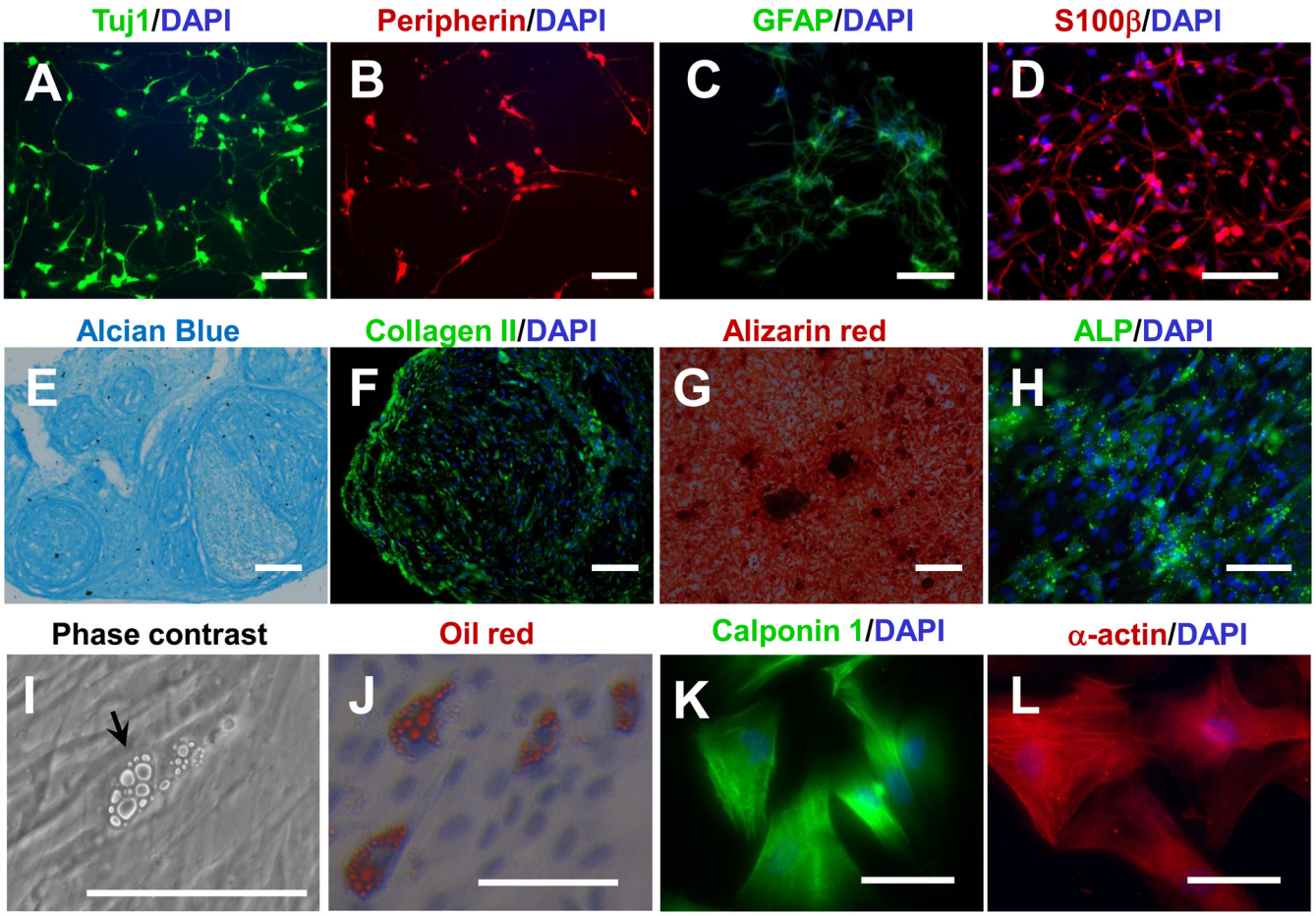

Figure 4.

In vitro differentiation of iPSC (BJ1-iPS1 line)-derived NCSCs into peripheral neural lineages (peripheral neurons, Schwann cells) and mesenchymal lineages (chondrocytes, osteoblasts, adipocytes and smooth muscle precursors). (**A–B**) Immunostaining for peripheral neuron markers Tuj1 (**A**) and peripherin (**B**). (**C–D**) Immunostaining for Schwann cell markers GFAP (**C**) and S100β (**D**). (**E–F**) Chondrogenic differentiation: Alcian blue staining for glycosaminoglycans (**E**) and immunofluorescent staining of collagen II (**F**). (**G–H**) Osteogenic differentiation: Alizarin red staining for calcified matrix (**G**) and immunofluorescent staining of alkaline phosphatase (ALP) (**H**). (**I–J**) Adipogenic differentiation: Phase contrast image (**I**) and oil red staining (**J**). (**K–L**) Immunostaining for smooth muscle markers calponin (**K**) and smooth muscle α-actin (**L**). In all immunofluorescence images, nuclei were stained by DAPI (in blue). Scale bars in **A, B, C, D, F, H, K and L** are 100 μm. Scale bars in **E, G, I and J** are 200 μm.

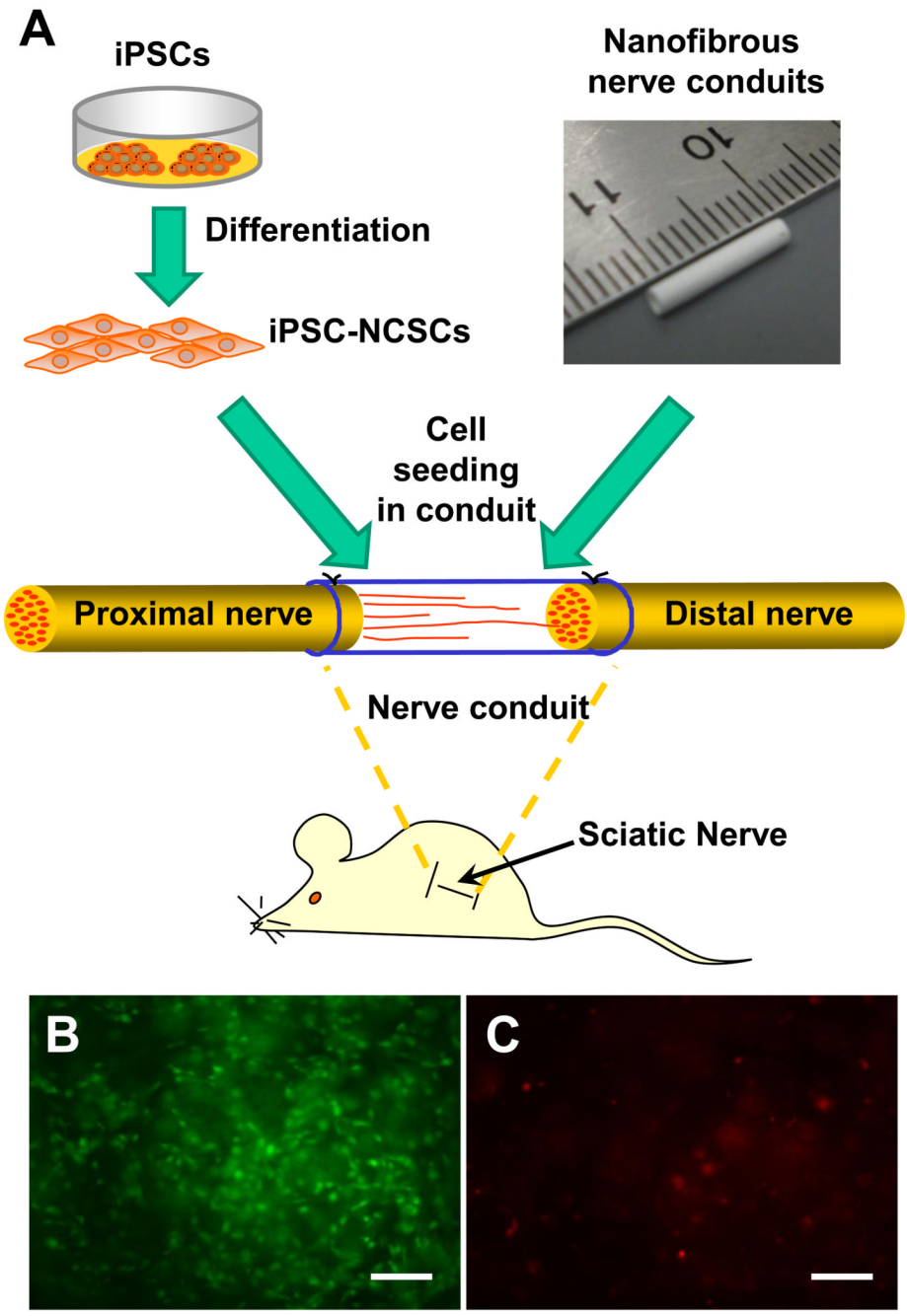

Figure 5.

Tissue engineered nanofibrous nerve conduits for peripheral nerve regeneration. (**A**) Schematic outline of tissue engineering approach by combining NCSCs and a nanofibrous nerve conduit. (**B–C**) The NCSCs were mixed with matrigel, injected in the nerve conduits, and cultured for one day in vitro. The viability of the cells was tested by using Live/dead assay. Live cells (calcein staining, in green) are shown in (**B**). Dead cells (ethidium homodimer-1 staining, in red) are shown in (**C**). Scale bars are 100 μm.

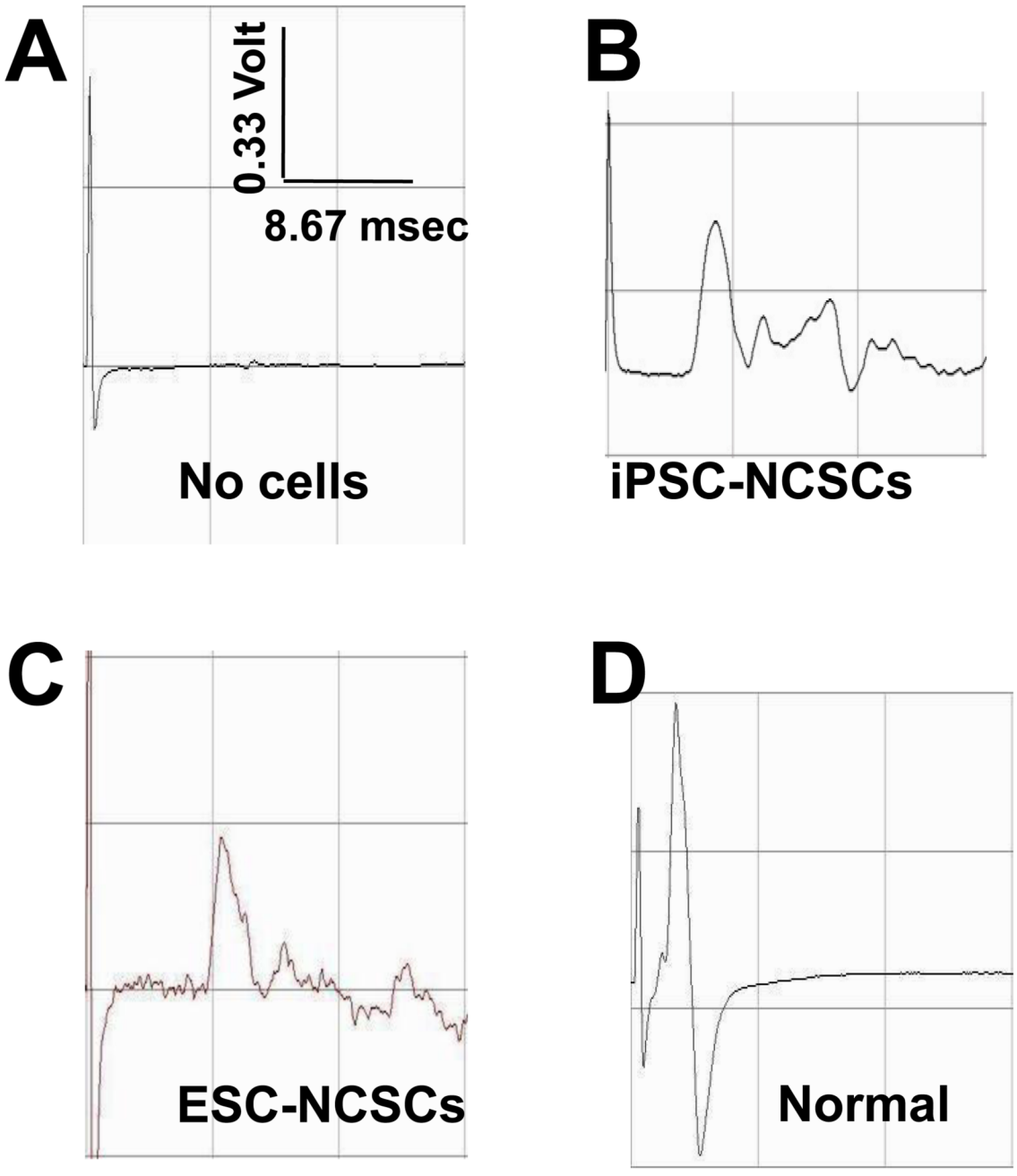

Figure 6.
Sciatic nerve regeneration by transplanting iPSC-derived NCSCs in nanofibrous nerve conduits. CMAP was measured at 1-month after surgery. Representative data are shown for the control group (without cells) (**A**), the group with iPSC-NCSC transplantation (**B**), the group with ESC-NCSC transplantation (**C**) and contralateral normal nerve group (**D**).

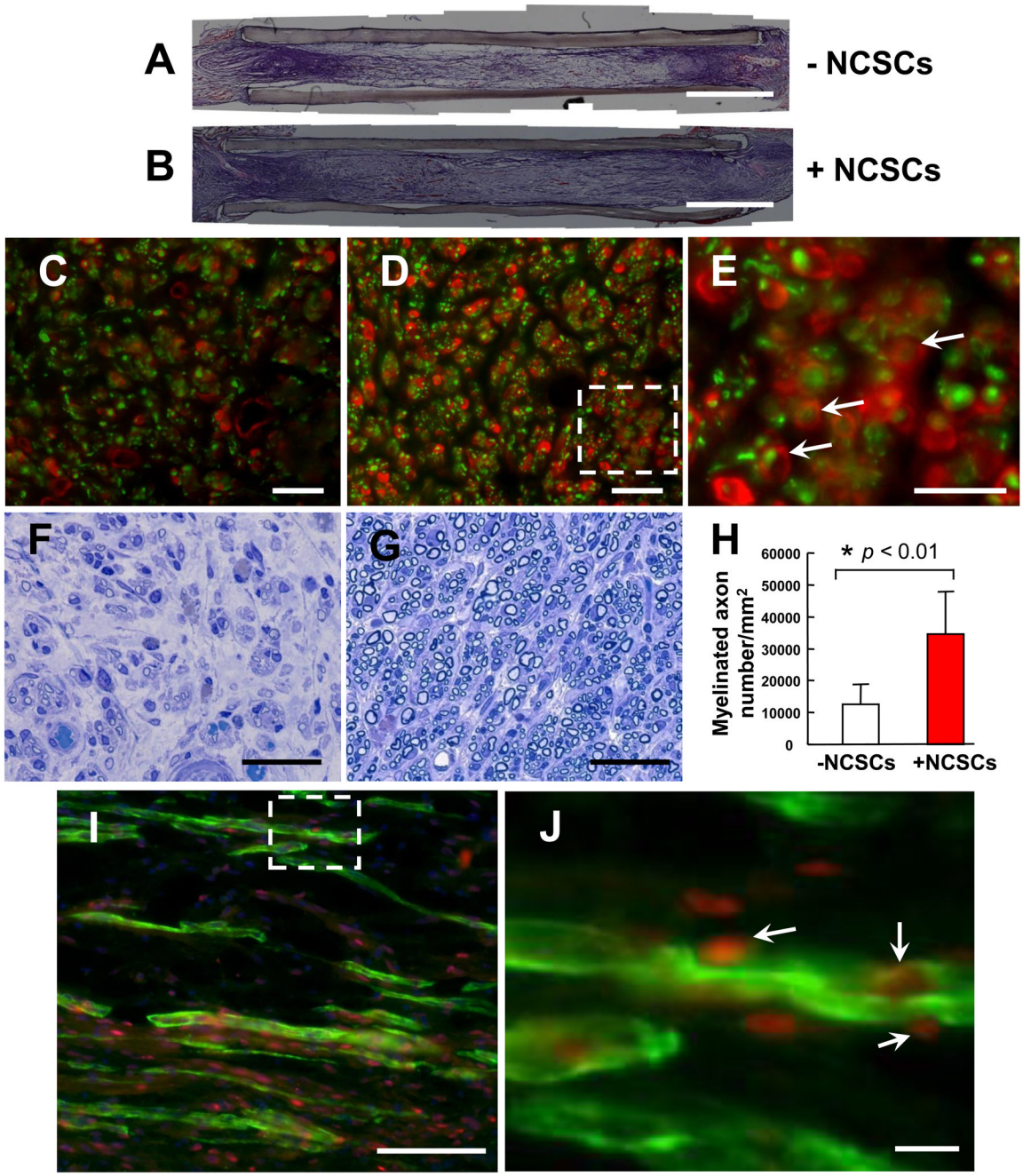

Figure 7.

NCSC differentiation in vivo. (**A–B**) Sciatic nerve tissue growth across the gap is achieved at 1 month time point. (**C–D**) Immunostaining of NF-M (green) and S100β (red) (cross sections at 5–7 mm from the proximal end) in the control group (**C**) and the group with iPSC-NCSC transplantation (**D**). A higher magnification of the inset area in (**D**) is shown in (**E**). Arrows indicate myelinated axons. (**F–G**) Toluidine blue staining of the regenerated nerve tissue (cross sections, 5–7 mm from the proximal end) in the control group (**F**) and the group with iPSC-NCSC transplantation (**G**). (**H**) The density of myelinated axons in the cross sections 5–7 mm from the proximal end. Bars represent mean ± standard deviation. * indicates significant difference ($p < 0.01$; n=5) compared to the control group. (**I**)

Immunofluorescence staining of Schwann cell marker S100β (Green) and human nuclei antigen NuMA (Red) in a longitudinal section of the iPSC (BJ1-iPS1) derived NCSC transplantation group. A higher magnification of the inset area in (**I**) is shown in (**J**). Arrows indicate the co-localization of S100β and NuMA. Scale bars in **C, D, F, G, J** = 10 μm; scale bar in **E** = 5 μm; scale bar in **I** = 100 μm.